

Target Mass Corrections to Electro-Weak Structure Functions and Perturbative Neutrino Cross Sections

S. Kretzer^{a,b} and M.H. Reno^c

^a*Physics Department, Brookhaven National Laboratory,
Upton, New York 11973, U.S.A.*

^b*RIKEN-BNL Research Center, Bldg. 510a, Brookhaven National Laboratory,
Upton, New York 11973 – 5000, U.S.A.*

^c*Department of Physics and Astronomy, University of Iowa
Iowa City, Iowa 52242 USA*

Abstract

We provide a complete and consistent framework to include subasymptotic perturbative as well as mass corrections to the leading twist ($\tau = 2$) evaluation of charged and neutral current weak structure functions and the perturbative neutrino cross sections. We revisit previous calculations in a modern language and fill in the gaps that we find missing for a complete and ready-to-use “NLO ξ -scaling” formulary. In particular, as a new result we formulate the mixing of the partonic and hadronic structure function tensor basis in the operator approach to deep inelastic scattering. As an underlying framework we follow the operator product expansion à la Georgi & Politzer that allows the inclusion of target mass corrections at arbitrary order in QCD and we provide explicit analytical and numerical results at NLO. We compare this approach with a simpler collinear parton model approach to ξ -scaling. Along with target mass corrections we include heavy quark mass effects as a calculable leading twist power suppressed correction. The complete corrections have been implemented into a Monte Carlo integration program to evaluate structure functions and/or integrated cross sections. As applications, we compare the operator approach with the collinear approximation numerically and we investigate the NLO and mass corrections to observables that are related to the extraction of the weak mixing angle from a Paschos-Wolfenstein-like relation in neutrino-iron scattering. We expect that the interpretation of neutrino scattering events in terms of oscillation physics and electroweak precision physics will benefit from our results.

I. INTRODUCTION

Recent neutrino experiments have shown strong evidence for neutrino masses and mixing. A variety of experiments [1, 2] have yielded data that when combined [3, 4] have led to a picture of neutrino mass and mixing with large mixings between $\nu_e \leftrightarrow \nu_\mu$ and $\nu_\mu \leftrightarrow \nu_\tau$, $\Delta m_{12}^2 \sim 7 \times 10^{-5} \text{ eV}^2$ and $\Delta m_{23}^2 \sim 2 \times 10^{-3} \text{ eV}^2$. Solar neutrinos are produced with $E_\nu < 20 \text{ MeV}$ [5], making $\nu_e \rightarrow \nu_\mu$ the relevant oscillation process. For the atmospheric case, $\langle E_\nu \rangle \sim 1 \text{ GeV}$ and $\nu_\mu \rightarrow \nu_\tau$ is the dominant oscillation process. The MINOS, OPERA and Chorus experiments will study $\nu_\mu \rightarrow \nu_\tau$ oscillations, either by ν_μ disappearance or ν_τ appearance [6].

In the GeV neutrino energy range, target mass effects are important. For muon neutrino charged current interactions, at low energies ($E_\nu \sim 100 - 800 \text{ MeV}$), the quasi-elastic process dominates and nucleon mass effects are easy to incorporate [7]. At intermediate energies, exclusive few pion production processes are the largest contributions to the cross section [8–10]. Above a few GeV, deep inelastic scattering (DIS) dominates the cross section. The energies for tau neutrino charged current interactions are higher because of the tau lepton threshold. A series of conferences (*NUINT*) has grown out of the efforts to improve and combine knowledge about the distinct neutrino interaction modes into event generation for oscillation searches [11].

In a different branch of recent research at the interface of neutrino physics and QCD, the NuTeV collaboration has measured the weak mixing angle from charged and neutral current muon neutrino and anti-neutrino interactions with a broad band beam (see Fig. 5). The beam flux maximum is at an energy of about $E_\nu \simeq 60 \text{ GeV}$ which translates into an average event energy of about $E_\nu \simeq 100 \text{ GeV}$ because the cross section rises approximately linearly with energy. NuTeV extracts a value of $\sin^2 \Theta_W = 0.2277 \pm 0.0013 \pm 0.0009$ [12] which lies about 3σ above the standard model value 0.2227 ± 0.00037 [13]. The latter fit value does not include neutrino scattering data. Possible explanations of the *NuTeV anomaly* within and beyond the standard model have been mapped out in Ref. [14]. Nuclear physics related complications in its interpretation - the NuTeV target material consists mostly of steel - have also been discussed in Ref. [15]. No consistent picture has as yet emerged from these efforts to understand the measured value.

The perturbative QCD parton picture is applicable at NuTeV energies and at the higher energy end of the oscillation neutrino beams. A perturbative background to (quasi-)elastic scattering is present at lower energies as well. At none of these energies can sub-asymptotic corrections to the simplest parton model picture be neglected, and both oscillation and precision neutrino physics are bound to benefit from a concise inclusion of these terms into data analysis. At least for precision physics, it does not suffice to model these corrections but it is a necessity to extract theory parameters using theoretically sound cross sections. E.g. a well defined separation of higher twist effects (see e.g. [16]) requires that power suppressed mass terms are accounted for correctly in the leading twist-2 cross section.

In the present article we include

- $\mathcal{O}(\alpha_s)$ perturbative QCD corrections
- $\mathcal{O}(M^n/Q^n)$ target mass effects
- $\mathcal{O}(m^n/Q^n)$ and $\mathcal{O}(\ln m^2/Q^2)$ heavy quark mass effects

- $\mathcal{O}(m_i^{2n}/(M^n E_i^n))$ heavy lepton mass effects (mostly for τ production)

and any combination of the above. One could summarize the above as (Nachtmann or Georgi & Politzer) ξ -scaling for weak structure functions merged with NLO QCD for light and heavy quarks: While the heavy quark and perturbative corrections come in through the expansion of the Wilson coefficients in the operator product expansion, the target mass corrections find their way into the final result through the Lorentz structure of the corresponding (non-reduced) operators.

Target mass corrections (TMC) to DIS have been known for a long time. The first discussion in terms of the operator product expansion (OPE) at leading order in QCD was done by Georgi and Politzer [17] in 1976. Later, these same target mass corrections were derived from a parton model point of view by Ellis, Furmanski and Petronzio [18]. DeRujula, Georgi and Politzer discussed next-to-leading order (NLO) QCD corrections to target mass corrected structure functions $W_{1,2}$ in the context of local duality in electroproduction [19] and using off-shell regularization. In this paper, we present the target mass corrections for charged current (CC) and weak neutral current (NC) ν_μ and ν_τ DIS with nucleons, including next-to-leading order QCD corrections and heavy quark production using modern conventions.

In the next Section, we outline the procedure for evaluating the TMC beyond leading order in QCD within the OPE. In Section III, we show our results in analytic form and compare them to the collinear parton model. We also make a few comments on nuclear targets and on the validity of the Albright & Jarlskog relations for the structure functions $F_{4,5}$. Numerical results for the structure functions are shown in Section IV for both the OPE and parton model approach to target mass corrections. As a further application, we evaluate observables that are related to the NuTeV Weinberg angle analysis in NLO QCD with high numerical precision. A summary appears in Section V.

II. TARGET MASS CORRECTIONS

A. Parton Model Approach (Briefly Revisited)

Target mass corrections appear in a number of ways that can be described in parton model language. First, the parton fraction ξ (Nachtmann variable [20]) of the light cone momentum of the nucleon $P_N^+ = (P_N^0 + P_N^z)/\sqrt{2}$ is related to the Bjorken x by

$$\frac{1}{\xi} = \frac{1}{2x} + \sqrt{\frac{1}{4x^2} + \frac{M^2}{Q^2}} \iff \xi = \frac{2x}{1 + \sqrt{1 + \frac{4M^2x^2}{Q^2}}} \quad (2.1)$$

for massless quarks. Second, there is a mixing between partonic structure functions in the evaluation of the hadronic structure functions. The partonic light cone momentum is related to the hadronic light cone momentum via $p^+ = \xi P_N^+$, however, partonic momentum projections are not simple rescalings of the hadronic momentum projections on the hadronic tensor $W^{\mu\nu}$ because $p^- \neq \xi P_N^-$ when $\{p^2, P_N^2\} = \{0, M^2\}$. Finally, in a collinear expansion [18] target mass effects appear from transverse momentum (k_T) effects.

In the collinear parton model ($k_T = 0$ approximation), target mass corrections have been evaluated in Ref. [21] and later in Ref. [22]. The intrinsic k_T of the target partons

is limited by the nucleon mass M , which introduces further corrections. Ellis, Furmanski and Petronzio [18] showed the equivalence of a non-collinear parton approach results, where the parton is on-shell but not collinear with the nucleon, to the operator product expansion target mass corrections, to which we will turn next.

B. Operator Product Expansion

The three contributions of the partonic approach appear automatically in the operator product expansion approach to target mass corrections, first discussed in this context by Georgi and Politzer [17]. In this approach, one starts with the relation between the hadronic tensor $W^{\mu\nu}$ and the virtual forward Compton scattering amplitude $T^{\mu\nu}$. For weak interactions, the relevant set of structure functions is W_i , $i = 1 - 5$:

$$W_{\mu\nu} \equiv \frac{1}{2\pi} \int e^{iq \cdot z} d^4z \langle N | [J_\mu(z), J_\nu(0)] | N \rangle \quad (2.2)$$

$$= \frac{1}{\pi} \text{Disc} \int e^{iq \cdot z} d^4z \langle N | iT(J_\mu(z)J_\nu(0)) | N \rangle \quad (2.3)$$

$$\equiv \frac{1}{\pi} \text{Disc} T_{\mu\nu} \quad (2.4)$$

$$= -g_{\mu\nu}W_1 + \frac{p_\mu p_\nu}{M^2}W_2 - i\epsilon_{\mu\nu\rho\sigma} \frac{p^\rho q^\sigma}{M^2}W_3 + \frac{q_\mu q_\nu}{M^2}W_4 + \frac{p_\mu q_\nu + p_\nu q_\mu}{M^2}W_5 . \quad (2.5)$$

In Eqs. (2.3), (2.4) the discontinuity is taken across the $\nu = q^0 > 0$ positive frequency cut:

$$\text{Disc} T_{\mu\nu} \equiv \lim_{\varepsilon \rightarrow 0} \frac{1}{2i} [T_{\mu\nu}(\nu + i\varepsilon) - T_{\mu\nu}(\nu - i\varepsilon)] . \quad (2.6)$$

The hadronic tensor $W_{\mu\nu}$ is probed in deep inelastic interactions with a leptonic current

$$J_\mu^l = \bar{\psi}_2 \gamma_\mu (v_l - a_l \gamma_5) \psi_1 \quad (2.7)$$

through exchange of a boson of virtuality Q^2 . The corresponding cross section in the target rest frame is

$$\frac{d^2\sigma^{\nu(\bar{\nu})}}{dx dy} = \frac{G_F^2 M E_\nu}{\pi(1 + Q^2/M_B^2)^2} \sum_{i=1}^5 w_i(x, y, E_\nu, v_l, a_l, m_1, m_2) F_i(x, Q^2) \quad (2.8)$$

where $M_{B=W^\pm, Z^0}$ is the boson mass, x and y are the standard DIS variables and where the modern normalizations are

$$\{F_1, F_2, F_3, F_4, F_5\} = \left\{ W_1, \frac{Q^2}{2xM^2}W_2, \frac{Q^2}{xM^2}W_3, \frac{Q^2}{2M^2}W_4, \frac{Q^2}{2xM^2}W_5 \right\} . \quad (2.9)$$

For purely electromagnetic interactions* we have

Interference contributions between γ^ and Z^0 at very high Q^2 (e.g. at HERA) are not sensitive to target mass corrections. They are, therefore, not covered by Eqs. (2.8), (2.10).

$$\frac{d^2\sigma^{l\pm}}{dx dy} = \frac{16\pi\alpha^2 ME_l}{Q^4} \sum_{i=1}^2 w_i(x, y, E_l, 1, 0, m_l, m_l) F_i(x, Q^2) . \quad (2.10)$$

The electroweak weights w_i in (2.8), (2.10) are listed in Eqs. (A1)-(A15) for general lepton masses and couplings along with the experimentally relevant cases.

As is well known, W_3 contributes only to weak processes because of the parity violating nature of the anti-symmetric ε -tensor. A sixth independent tensor combination $\sim W_6(p_\mu q_\nu - p_\nu q_\mu)$ does not couple to the the most general leptonic current

$$L^{\mu\nu}(v_l, a_l, m_1, m_2)(p_\mu q_\nu - p_\nu q_\mu) = 0 \quad \forall\{v_l, a_l, m_1, m_2\} \quad (2.11)$$

where $L^{\mu\nu}$ is the leptonic analogue of the hadronic $W_{\mu\nu}$. Because W_6 decouples from the DIS process, we omit it from the beginning and throughout.

In neutral current reactions, $W_{4,5}$ contribute through the axial coupling a_l only, i.e. they do not couple to a γ^* exchange. In standard formulae, the tensors corresponding to W_4 and W_5 are sometimes combined with those corresponding to W_1 and W_2 so that current conservation is manifest in the electromagnetic case. Generally, for both neutral and charged current weak reactions the structure functions W_4 and W_5 do not appear in the usual discussion since they are multiplied by the ratio of the lepton mass squared to ME_ν . They obey the Albright-Jarlskog relations [23] which are valid at leading order in the limit of massless quarks and a massless target[†]:

$$F_4 = 0 \quad (2.12)$$

$$2xF_5 = F_2 \quad (2.13)$$

The forward scattering amplitude, explicitly including perturbative corrections, can be written as

$$T^{\mu\nu} = \sum_{k=1}^{\infty} \left(-g^{\mu\nu} q_{\mu_1} q_{\mu_2} C_1^{2k} + g_{\mu_1}^\mu g_{\mu_2}^\nu Q^2 C_2^{2k} - i\epsilon^{\mu\nu\alpha\beta} g_{\alpha\mu_1} q_\beta q_{\mu_2} C_3^{2k} \right. \\ \left. + \frac{q^\mu q^\nu}{Q^2} q_{\mu_1} q_{\mu_2} C_4^{2k} + (g_{\mu_1}^\mu q^\nu q_{\mu_2} + g_{\mu_1}^\nu q^\mu q_{\mu_2}) C_5^{2k} \right) q_{\mu_3} \dots q_{\mu_{2k}} \frac{2^{2k}}{Q^{4k}} A_{2k} \Pi^{\mu_1 \dots \mu_{2k}} , \quad (2.14)$$

where A_{2k} represents the reduced (scalar) matrix element of a twist-2 (traceless and symmetric) operator $\mathcal{O}_{\tau=2}^{\mu_1 \dots \mu_{2k}}$ of spin $2k$

$$\langle N | \mathcal{O}_{\tau=2}^{\mu_1 \dots \mu_{2k}} | N \rangle = A_{2k} \Pi^{\mu_1 \dots \mu_{2k}} . \quad (2.15)$$

The QCD perturbative corrections come in through non-trivial Wilson coefficients C_i^{2k} . In Eq. (2.14), the factorization into universal operator matrix elements and process-dependent coefficient functions is a consequence of the operator product expansion[‡] [24] of the product

[†]The conditions under which Eqs. (2.12) and (2.13) are valid individually are detailed in the appendix of Ref. [22] and in Section IIID 2 below.

[‡]The OPE has found its way into many excellent textbooks and clear pedagogical introductions can be found in e.g. [25].

of currents $T^{\mu\nu}$ in Eq. (2.3). We assume that $\mathcal{O}_{\tau=2}^{\mu_1 \dots \mu_{2k}}$ is of twist 2 to make contact with the parton model. For the following evaluation of the target mass corrections, however, it is sufficient that \mathcal{O} is a traceless and symmetric operator. Symmetry under permutation and tracelessness under contraction of any pair of indices of $\mathcal{O}_{\tau=2}^{\mu_1 \dots \mu_{2k}}$ require then that the tensor part of the matrix element in Eq. (2.15) is

$$\Pi^{\mu_1 \dots \mu_{2k}} = \sum_{j=0}^k (-1)^j \frac{(2k-j)!}{2^j (2k)!} \underbrace{g \dots g}_j \underbrace{p \dots p}_{(2k-2j)} (p^2)^j, \quad (2.16)$$

where $g \dots g p \dots p$ abbreviates a sum over $(2k)!/[2^j j! (2k-2j)!]$ permutations (not counting identical terms such as $g^{\mu_i \mu_j} = g^{\mu_j \mu_i}$ twice) of the indices. In Eq. (2.16) the $j=0$ approximation $\Pi^{\mu_1 \dots \mu_{2k}} \propto p^{\mu_1} \dots p^{\mu_{2k}}$ reproduces the massless parton model and the $j>0$ terms resum the target mass corrections. While they are formally power suppressed of order $\mathcal{O}(M^{2k}/Q^{2k})$, the corrections derive from the same operators $\mathcal{O}_{\tau=2}^{\mu_1 \dots \mu_{2k}}$ as the $j=0$ term and as such are of twist-2. This is in contrast to power corrections from operators of higher twist $\mathcal{O}_{\tau>2}^{\mu_1 \dots \mu_{2k}}$ which introduce new non-perturbative matrix elements independent of those in Eq. (2.15). In classical terminology twist classifies strictly the dimension minus the spin of an operator; the difference between target mass corrections and higher twists is, nevertheless, sometimes referred to as a distinction between kinematic and dynamical higher twists as well.

The quantity A_{2k} is the $2k^{\text{th}}$ moment of a universal function f or the $(2k-1)^{\text{th}}$ moment of the quark distributions $q(x)$ [§]

$$A_{2k} = \int_0^1 dx x^{2k} f(x, Q^2) = \int_0^1 dx x^{2k-1} q(x, Q^2). \quad (2.17)$$

Beyond leading order we include the non-universal Wilson coefficients into the moment integral

$$C_i^{2k} A_{2k} = \int_0^1 dx x^{2k} f_i(x, Q^2), \quad (2.18)$$

thus defining a set of non-universal x -space functions $f_{i=1, \dots, 5}$. The f_i can be related to the zero mass limit $F_i^{(0)}$ of the experimental structure functions F_i from the $j=0$ term of the series (2.16) as will be explained in the next section; the effect of the resummation of the $j>0$ terms will induce convolution integrals over the $F_i^{(0)}$ and lead to Nachtmann scaling [20].

The standard calculation à la Georgi-Politzer of extracting the moments of the structure functions, then performing inverse Mellin transforms, leads to equations most simply expressed in terms of $f_i(\xi, Q^2)$ and

[§]For ease of notation, throughout this article we sometimes suppress scale dependence as a functional argument. Q^2 -dependence enters through the renormalization of $\mathcal{O}_{\tau=2}^{\mu_1 \dots \mu_{2k}}$; i.e. strictly $A_{2k} = A_{2k}(Q^2)$. Also, for the purpose of this article and in order to make contact with the parton model it suffices to assume that $\mathcal{O}_{\tau=2}^{\mu_1 \dots \mu_{2k}}$ is a quark operator since the inclusion of operators built from gluons and operator mixing would not alter the discussion anywhere.

$$h_i(\xi, Q^2) = \int_{\xi}^1 d\xi' f_i(\xi', Q^2) \quad (2.19)$$

$$g_i(\xi, Q^2) = \int_{\xi}^1 d\xi' h_i(\xi', Q^2) = \int_{\xi}^1 d\xi' (\xi' - \xi) f_i(\xi', Q^2). \quad (2.20)$$

The middle part of Eq. (2.20) is a more transparent representation when we write down the results below. For numerical evaluation, however, it is more convenient to express the double convolution integral as a moment of a single convolution as suggested by the right-hand-side of the same equation.

We have extended the Georgi-Politzer [17] and DeRujula-Georgi-Politzer [19] analyses by including the full set of weak structure functions along with their Wilson coefficients C_i^{2k} . Abelian gauge invariance is not assumed through *a priori* relations among C_i^{2k} , although it is restored in the electromagnetic scattering case by the explicit values of C_i^{2k} . In unpolarized DIS, the leading component is of twist-2 for any $W_{i=1,\dots,5}$, and the coefficient functions do the bookkeeping of the tensor components in $W_{\mu\nu}$. One finds a mixing of structure functions, which for F_1 was already found in Ref. [19]. The general pattern of mixing can be easily inferred from the $j > 0$ terms in Eq. (2.16) that add different tensor components to the $j = 0$ term. We note that in polarized DIS, the spin dependent structure functions [26–29] g_1 and g_2 receive contributions from twist-2 and twist-2 and 3 operators, respectively. In this case, tracking the Wilson coefficient basis follows automatically from tracking the operators of twist two and three and from the Wandzura-Wilczek relation for the twist-2 part [30].

The method of evaluating target mass corrections as inverse Mellin transforms of moments of structure functions was presented in explicit detail in the Georgi & Politzer analysis [17] already. Recent analogous calculations in the spin dependent case [28, 29] have repeated the mathematical steps involved. Apart from the differences listed above, we feel it is unnecessary to add a further derivation to the literature. In the next section, we show our explicit results for the target mass corrected structure functions W_i and the corresponding F_i .

III. RESULTS

A. Generic Formulae

The procedure outlined above leads directly to the results for the structure functions in terms of Bjorken x , the Nachtmann variable ξ , and Q^2 as well as $\mu \equiv M^2/Q^2$. The structure functions are:

$$W_1 = \frac{1}{2} \frac{\xi}{1 + \mu\xi^2} f_1(\xi, Q^2) - \mu x^2 \frac{\partial}{\partial x} \left[\frac{g_2(\xi, Q^2)}{1 + \mu\xi^2} \right] \quad (3.1)$$

$$W_2 = 2\mu x^3 \frac{\partial^2}{\partial x^2} \left[\frac{x g_2(\xi, Q^2)}{\xi(1 + \mu\xi^2)} \right] \quad (3.2)$$

$$W_3 = -\mu x^2 \frac{\partial}{\partial x} \left[\frac{h_3(\xi, Q^2)}{(1 + \mu\xi^2)} \right] \quad (3.3)$$

$$W_4 = \frac{\mu\xi}{2(1 + \mu\xi^2)} f_4(\xi, Q^2) + 2\mu^2 x^2 \frac{\partial}{\partial x} \left[\frac{\xi h_5(\xi, Q^2)}{1 + \mu\xi^2} \right] + 2\mu^3 x^3 \frac{\partial^2}{\partial x^2} \left[\frac{\xi^2 g_2(\xi, Q^2)}{(1 - \mu\xi^2)(1 + \mu\xi^2)} \right] \quad (3.4)$$

$$W_5 = -\mu x^2 \frac{\partial}{\partial x} \left[\frac{h_5(\xi, Q^2)}{(1 + \mu \xi^2)} \right] - 2\mu^2 x^3 \frac{\partial^2}{\partial x^2} \left[\frac{\xi g_2(\xi, Q^2)}{(1 - \mu \xi^2)(1 + \mu \xi^2)} \right] \quad (3.5)$$

After performing the derivatives in Eqs. (3.1)-(3.5), one gets a generic form

$$W_j = \sum_{i=1,5} a_j^i f_i(\xi, Q^2) + b_j^i h_i(\xi, Q^2) + c_j g_2(\xi, Q^2) . \quad (3.6)$$

The generic formula for the W_j applicable to Eq. (2.5) is more useful translated to modern normalization conventions of the structure functions (F_j) or to the parton model language. In the next sections, we associate the f_i and related h_i and g_2 to the experimental structure functions $F_i(x, Q^2)$ in the $M \rightarrow 0$ limit. The $F_i(x, Q^2)|_{M=0}$ can be evaluated at NLO using parton distribution functions as documented in detail in [22, 31]. As in [22] and as is appropriate for the neutrino energies under consideration, we will be working in the $\overline{\text{MS}}$ factorization scheme with $n_f = 3$ active flavours. To avoid redundancy, we will not reproduce the formulae of [22, 31] in the present article. In Section III C we comment on nuclear target corrections. We then consider the association of W_j to parton distribution functions in Section III D. The master formulae for F_j in structure function language and in parton model language appear in Eqs. (3.17) and (3.27) below.

B. Target Mass Corrected Structure Functions

Our procedure for determining the quantities f_i and associated h_i and g_i is to consider the experimental structure functions F_i in Eq. (2.9) with the W_i in Eqs. (3.1)-(3.5) in the $\mu \rightarrow 0$ limit

$$F_i^{(0)} \equiv F_i|_{M=0} , \quad (3.7)$$

in which $\xi \rightarrow x$. Note that the $F_i^{(0)}$ here denote functional forms and not observables – though they are accessible in principle through the inversion of Eq. (3.17) below as the structure functions with moments of definite spin in the Nachtmann sense [20] or the perturbatively corrected scaling functions in the duality sense [19]. To make the distinction from $F_i^{(0)}$ more obvious we will, below, sometimes label the measurable structure functions F_i^{TMC} . From the $j = 0$ term of the target mass series in Eq. (2.16) we find the following relations between f_i and the zero-target-mass limit functions $F_i^{(0)}$

$$\left\{ F_1^{(0)}(x), F_2^{(0)}(x), F_3^{(0)}(x), F_4^{(0)}(x), F_5^{(0)}(x) \right\} = \left\{ \frac{x}{2} f_1(x), x^2 f_2(x), x f_3(x), \frac{x}{4} f_4(x), \frac{x}{2} f_5(x) \right\} . \quad (3.8)$$

In Section III.C, we show that this form explicitly substantiates the partonic interpretation

$$f_i(x) = k_i f(x) + \mathcal{O}(\alpha_s) = k_i \frac{q(x)}{x} + \mathcal{O}(\alpha_s) \quad (3.9)$$

with the couplings of the quark current

$$J_\mu^q = \bar{\psi}_2 \gamma_\mu (v_q - a_q \gamma_5) \psi_1 \quad (3.10)$$

entering as

$$\begin{aligned}
k_i &= v_q^2 + a_q^2 \quad (i=1,2,5) \\
k_i &= 2 v_q a_q \quad (i=3) \\
k_i &= 0 \quad (i=4) .
\end{aligned}$$

The form of Eq. (3.9) is modified slightly to include quark masses. For the applications in Section IV we calculate the $F_j^{(0)}$ using the $\mathcal{O}(\alpha_s)$ coefficient functions in Refs. [22, 31]. Here we focus on relating F_i^{TMC} to the $F_j^{(0)}$ and their convolutions. With Eq. (3.8), Eqs. (2.19) and (2.20) now become

$$h_1(\xi, Q^2) = \int_{\xi}^1 d\xi' \frac{2F_1^{(0)}(\xi', Q^2)}{\xi'} \quad (3.11)$$

$$h_2(\xi, Q^2) = \int_{\xi}^1 d\xi' \frac{F_2^{(0)}(\xi', Q^2)}{\xi'^2} \quad (3.12)$$

$$h_3(\xi, Q^2) = \int_{\xi}^1 d\xi' \frac{F_3^{(0)}(\xi', Q^2)}{\xi'} \quad (3.13)$$

$$h_4(\xi, Q^2) = \int_{\xi}^1 d\xi' \frac{4F_4^{(0)}(\xi', Q^2)}{\xi'} \quad (3.14)$$

$$h_5(\xi, Q^2) = \int_{\xi}^1 d\xi' \frac{2F_5^{(0)}(\xi', Q^2)}{\xi'} \quad (3.15)$$

$$g_2(\xi, Q^2) = \int_{\xi}^1 d\xi' h_2(\xi', Q^2) = \int_{\xi}^1 d\xi' (\xi' - \xi) \frac{F_2^{(0)}(\xi', Q^2)}{\xi'^2} \quad (3.16)$$

From Eqs. (3.1)-(3.5), (3.8), (2.9), (3.11)-(3.16), the target mass corrected structure functions then are

$$F_j^{TMC} = \sum_{i=1,5} A_j^i F_i^{(0)}(\xi, Q^2) + B_j^i h_i(\xi, Q^2) + C_j g_2(\xi, Q^2) . \quad (3.17)$$

The coefficients $\{A_j^i, B_j^i, C_j\}$ are listed in Table I-III in terms of x , ξ , μ and ρ where

$$\rho \equiv \frac{1 + \mu\xi^2}{1 - \mu\xi^2} = \sqrt{1 + 4\mu x^2} . \quad (3.18)$$

Note that

$$x = \frac{\xi}{1 - \mu\xi^2} . \quad (3.19)$$

While we have sometimes referred to twist-2 operators to meet the parton model, Eq. (3.17) holds for contributions from any traceless and symmetric operators and it is independent of the perturbative order in α_s . For leading order $\mathcal{O}(\alpha_s^0)$ twist-2 coefficient functions, $F_{1,2}$ as in Eq. (3.17) agree with the standard results in Ref. [17] and the non-collinear parton results in Ref. [18]. For F_3 there is a factor of $2x$ mismatch in relative normalization of the $F_3^{(0)}$ and h_3 term between Ref. [17] and Ref. [18]; we agree with the results in Ref. [18].

C. A Note on Nuclear Targets

By the very nature of weak interactions heavy nuclei are more natural targets than a nucleon, so a brief comment on large $M_A = AM_N$ nuclei may be worthwhile. In the OPE the coefficient functions are manifestly target independent and the target dependence resides in a generalization of Eq. (2.15) with $|N\rangle$ replaced by a general nuclear target

$$\langle Z, A | \mathcal{O}_{\tau=2}^{\mu_1 \dots \mu_{2k}} | Z, A \rangle = A_{2k}^{(Z,A)} \Pi^{\mu_1 \dots \mu_{2k}} . \quad (3.20)$$

i.e. ultimately the nuclear dependence for $\tau = 2$ is contained in nuclear modifications of the PDF in Eq. (2.17)**

$$A_{2k}^{(Z,A)} = A \int_0^1 dx x^{2k-1} q^{(Z,A)}(x, Q^2) . \quad (3.21)$$

Genuine higher twist $\tau > 2$ effects may be of different relative size in nuclei, e.g. the twists investigated in Ref. [32] are enhanced by a factor $A^{1/3}$. The $M_A^2 = A^2 M_N^2$ enhancement of target mass terms is, however, balanced everywhere by kinematic factors that scale with inverse powers of A such as

$$x_A = \frac{Q^2}{2P_A \cdot q} = \frac{Q^2}{2AP_N \cdot q} = \frac{x}{A} \quad (3.22)$$

Neglecting for the moment the nuclear modifications in Eq. (3.21), under the assumption that††

$$q^{(Z,A)}(x) = A q(x) \Theta(1 - x) \quad (3.23)$$

target mass corrections are then the same for nuclear targets. Eq. (3.23) neglects the large $1 < x < A$ tail in nuclei which is (small but) nonzero due to Fermi motion.

D. Comparison with the Collinear Parton Model

So far, no reference to the parton model was required in deriving the results. It is interesting to compare the above results, derived from the operator product expansion, with the collinear ($\vec{k}_\perp = \vec{0}$) parton model approach to target mass corrections [21, 22]. The latter also leads to Nachtmann scaling but the mixing of the tensor basis comes in only from the non-collinear $k^- \neq \xi P^-$ component of the parton momentum. This approximation avoids single and double-convolution terms of the form of Eqs. (3.11)-(3.16). If the collinear approximation turns out to be of reasonable accuracy, one may hope to employ similarly approximate mass corrections to processes where the rigorous operator approach is not available such as processes where the final state is not fully inclusive.

**In the absence of nuclear effects we could drop the label “ Z, A ” on $q^{(Z,A)}$ in Eq. (3.21).

††The isospin orientation is attributed to the PDF without explicit labeling.

1. The CC Process including Charm Production

We now find relations between f_i and \mathcal{F}_i , the parton model structure functions for scattering off of the Cabibbo-Kobayashi-Maskawa-rotated weak eigenstates (e.g., $d' = |V_{d,u}|^2 d + |V_{s,u}|^2 s$), normalized such that for ν scattering at leading order in QCD, $\mathcal{F}_i = (1 - \delta_{i4})(d' + \dots)$. The full expressions for \mathcal{F}_i appear in, for example, Eq. (10) of Ref. [22]. To include charm production, we introduce the parameter $\lambda \equiv Q^2/(Q^2 + m_c^2)$ (i.e. one should simply set $\lambda \rightarrow 1$ for the light quark contributions). Our result is that

$$f_{1,3,5}(\xi, Q^2) = \frac{2\mathcal{F}_{1,3,5}(\xi, Q^2)}{\xi} \quad (3.24)$$

$$f_2(\xi, Q^2) = \frac{2\mathcal{F}_2(\xi, Q^2)}{\lambda\xi} \quad (3.25)$$

$$f_4(\xi, Q^2) = \frac{4\mathcal{F}_4(\xi, Q^2)}{\xi}. \quad (3.26)$$

To make contact with the measurable structure functions F_i , we instead write our results in terms of the partonic functions \mathcal{F}_i and convolutions:

$$F_j^{\text{TMC}} = \sum_{i=1,5} \alpha_j^i \mathcal{F}_i(\xi, Q^2) + \beta_j^i \mathcal{H}_i(\xi, Q^2) + \gamma_j \mathcal{G}_2(\xi, Q^2). \quad (3.27)$$

The quantities \mathcal{H}_i and \mathcal{G}_i are

$$\mathcal{H}_i(\xi, Q^2) = \int_{\xi}^1 d\xi' \frac{\mathcal{F}_i(\xi', Q^2)}{\xi'} \quad (3.28)$$

$$\mathcal{G}_i(\xi, Q^2) = \int_{\xi}^1 d\xi' \mathcal{H}_i(\xi', Q^2) \quad (3.29)$$

The coefficients α_j^i , β_j^i and γ_j are listed in Tables IV-VI.

As can be seen from Table IV, the α_j^i coefficients are mostly diagonal, however, there is some mixing of the parton functions \mathcal{F}_i for F_4 and F_5 . This was already seen in our analysis that included target mass effects in the collinear limit. In fact the terms $\sum_i \alpha_j^i \mathcal{F}_i$ contributions to F_i in Eq. (3.27) are a factor of $1/(1 + \mu\xi^2)$ suppressed relative to our earlier results Eqs. (14)-(18) in Ref. [22] which included target mass corrections in the collinear limit. The k_T corrections are also responsible for the remaining terms proportional to \mathcal{H}_i and \mathcal{G}_2 in Eq. (3.27).

2. Massless Quark Limit and the NC Process

Finite charm mass effects are mostly important at intermediate energies. For low energy processes, charm production is a negligible effect, whereas at very high energies, charm can be treated effectively massless. In these limits, we can evaluate the target mass corrections assuming three or four massless quarks. Only three independent helicity amplitudes survive the limit of massless quarks, or more generally the limit where the quark fields that build the currents in Eq. (2.2) are mass-degenerate. This is discussed in the appendix of Ref. [22]. For massless quarks in CC interaction, or generally for the NC interaction we then have:

$$\mathcal{F}_5 = \mathcal{F}_2 \quad (3.30)$$

$$\mathcal{F}_4 = \frac{1}{2}(\mathcal{F}_2 - \mathcal{F}_1) \quad (3.31)$$

so $f_5 = f_2$ and $f_4 = f_2 - f_1$. Given these relations, one finds that

$$W_4 = -\mu W_1 + \frac{1}{4x^2} W_2 \quad (3.32)$$

$$W_5 = \frac{1}{2x} W_2 \quad (3.33)$$

which lead, with the usual definitions, to the expressions

$$F_4 = \frac{1}{2} \left[\frac{F_2}{2x} - F_1 \right] \quad (3.34)$$

$$F_5 = \frac{1}{2x} F_2, \quad (3.35)$$

where all structure functions are understood to be including the target mass corrections of Eq. (3.17). Thus, in the massless quark limit for CC interactions, or for the NC process, the evaluation of F_1 , F_2 and F_3 is sufficient to fully describe the target mass corrections, even when lepton masses cannot be neglected compared to the incident neutrino energy.

IV. APPLICATIONS

A. Operator Product Expansion versus Collinear Parton Model

We have already commented on the comparison between the ξ scaling corrections derived from the OPE and those obtained in the collinear parton model in Section III D. In this section we parallel this discussion with a numerical evaluation of the charged current neutrino scattering structure functions F_2 and F_3 in both of these approaches.

Figs. 1-4 show results of F_2 and F_3 at $Q^2 = 1$ and 4 GeV². The figures 1-4 (a) show the absolute scale of the structure functions, while Figs. 1-4 (b) show ratios of structure functions. With (a) and (b) together, one can avoid overstressing kinematic regions with large corrections which are, nevertheless, not relevant because the value of the structure function is small. The structure functions in the figures are evaluated using the GRV parton distribution functions [33], which have 3 active flavors. Here and below, we work in the convention of three active flavors and in the $\overline{\text{MS}}$ factorization scheme.

Fig. 1 (a) shows F_2 at $Q^2 = 1$ GeV² as a function of x . The solid curve is our full result of target mass corrected NLO (ξ scaling corrections derived from the OPE) $F_2(\xi, 1 \text{ GeV}^2)$. The dot-dashed curve is the NLO corrected $F_2^{(0)}(x, 1 \text{ GeV}^2)$ without TMC, and the dashed curve is the LO $F_2^{(0)}$.

In Fig. 1 (b), we show ratios of F_2 's at $Q^2 = 1$ GeV², all as a function of x . The solid line shows the ratio of the LO $F_2(\xi, 1 \text{ GeV}^2)$ evaluated with the full TMC to the collinear approximated TMC (TMC-COL) corrected F_2 . The collinear approximation is discussed in Ref. [22] and is summarized by

$$F_j = \sum_{i=1,\dots,5} \alpha_j^i (2 - \xi/x) \mathcal{F}_i(\xi, Q^2). \quad (4.1)$$

The dot-dashed line is the ratio of the full TMC corrected F_2 to the TMC-COL F_2 , both at NLO. One finds that the collinear approximation does reasonably well in representing the full TMC structure function F_2 .

The dashed line in Fig 1 (b) is the ratio of the NLO TMC F_2 to the NLO F_2 in the $M \rightarrow 0$ limit ($F_2^{(0)}$). The TMC are of order 15% at $x = 0.4$ and very large above $x \sim 0.7$. The region $x > 0.7$ is where the NLO $F_2^{(0)}$ is less than 10% of its value at $x = 0.1$.

Figs. 2 (a) and 2 (b) show the same quantities for $Q^2 = 4 \text{ GeV}^2$. Figs. 3 (a), 3 (b) and 4 (a), 4 (b) are the corresponding results for F_3 .

The comparative results may be summarized as follows

- As is well known, target mass corrections become important at low Q and they are suppressed at low x .
- For $0 < x < 0.9$, the collinear approximation deviates from the exact OPE results by at most 10% for F_2 and at most 20% for F_3 . A more detailed examination of the adequacy of the collinear approximation for phenomenology will be left to future work.

As briefly mentioned above, the second point may be reason for some optimism (though by no means a proof) that simple kinematic rescalings provide the dominant hadron mass effects in other processes as well. A crucial observation here is that a rescaling term is enhanced by a derivative factor

$$F(\xi) - F(x) = \frac{1}{2} \left. \frac{dF}{d\xi} \right|_{\xi=x} (\xi - x) + \dots = \mathcal{O}\left(\frac{M^2}{Q^2}\right) F'(x) \quad (4.2)$$

for a steeply falling function $F(\xi)$. E.g. for a toy function $F(x) \propto (1-x)^\beta$ the rescaling for $x \rightarrow 1$ is enhanced as $1/(1-x)$ compared to a multiplicative $[1 + \mathcal{O}(\frac{M^2}{Q^2})]F(x)$ correction term.

B. The Paschos-Wolfenstein Relation and Related Observables

In the following, integrated cross sections

$$\sigma_{\text{NC,CC}}^{\nu,\bar{\nu}} = \frac{\int dE_{\nu,\bar{\nu}} d\sigma_{\text{NC,CC}}^{\nu,\bar{\nu}} \Phi(E_{\nu\bar{\nu}}) \big|_{20 \text{ GeV} < y E_{\nu,\bar{\nu}} < 180 \text{ GeV}}}{\int dE_{\nu,\bar{\nu}} \Phi(E_{\nu\bar{\nu}})} \quad (4.3)$$

will refer to flux-averaged integrals with a cut on hadronic energy as in the experimental analysis [12]. We use the (anti-)neutrino fluxes in a step function form as shown in Fig 5. We will consider the *counting experiment* observables

$$R^{\nu,\bar{\nu}} \equiv \frac{\sigma_{\text{NC}}^{\nu,\bar{\nu}}}{\sigma_{\text{CC}}^{\nu,\bar{\nu}}} \quad (4.4)$$

as well as the Paschos-Wolfenstein [35] relation

$$R^- \equiv \frac{\sigma_{\text{NC}}^\nu - \sigma_{\text{NC}}^{\bar{\nu}}}{\sigma_{\text{CC}}^\nu - \sigma_{\text{CC}}^{\bar{\nu}}} \simeq \frac{1}{2} - \sin^2 \Theta_{\text{W}} \quad (4.5)$$

The question to what extent the approximation in Eq. (4.5) holds in the light of the high precision data of Ref. [12] has been of some debate recently. For an ideally iso-scalar target and under the neglect of charm production components one has that $R^- = 1/2 - \sin^2 \Theta_{\text{W}}$ at arbitrary order in QCD as long as there are no $(s - \bar{s})(x)$ component in the nucleon strange sea [14]. For definiteness, we will consider the scattering of neutrinos on an $Z = 26, A = 56$ iron target and charm production with $m_c = 1.3$ GeV. We will be using parton distributions [33, 34] from the literature, though, which do not contain a $(s - \bar{s})(x)$ asymmetry. In a somewhat idealized Mellin moment language, NLO corrections have already been estimated in Ref. [14] and we refer the reader to this reference^{‡‡} for more detailed background information. Our evaluation of Eqs. (4.4), (4.5) complements Ref. [14] in that we do not make the approximations required for a moment analysis and that we mimic the experimental setup to some extent by including the neutrino flux and hadronic energy cut in Eq. (4.3). Technically, Eq. (4.3) is evaluated as a 5-dimensional Monte Carlo integral:

$$\int d\sigma dE_{\nu, \bar{\nu}} \propto \int dx dy dE_{\nu, \bar{\nu}} d\xi_{1,2} \quad (4.6)$$

over the kinematic variables and two convolution variables arising from NLO and TM correction integrals. Eq. (4.6) integrates numerically over plus type distributions in the perturbative coefficient functions. In a MC integral, this has to be done with care to achieve the required accuracy.

Our results for $R^{\nu, \bar{\nu}}$ are summarized in Table VII for two sets (GRV [33] and CTEQ6 [34]) of parton distribution functions, for a LO^{§§} or NLO evaluation and for the standard model and the anomalous value of the Weinberg angle. The CTEQ6 parton distribution analysis also provides a master formula – Eq. (3) in [34] – to estimate the PDF related error on a physical observable through a set of error PDFs. Our results can be summarized as follows

- $R^{\bar{\nu}}$ is insensitive to the Weinberg angle and sensitive to NLO corrections
- R^ν is insensitive to NLO corrections within its sensitivity to the Weinberg angle
- The impact of PDF uncertainties from pre-determined PDF fits is inconclusive, e.g. the error estimate of CTEQ6 for R^ν does not overlap with the evaluation based on GRV. This fact is not too surprising, though, given there are other factors such as scheme (number of active flavours) uncertainties and that the error estimate has not been tailored to match this particular high precision application.

^{‡‡}While completing this article the effect of NNLO moments were presented in Ref. [36].

^{§§}The LO evaluation also neglects target mass effects. The charm mass is kept non-zero along the LO slow rescaling prescription.

From these results, one cannot derive a conclusive estimate of the impact of NLO corrections on the analysis [12] and further work will be required. For now, we will restrict ourselves to playing the game to treat Eq. (4.5) as a would-be identity and to solve it for the Weinberg angle:

$$\left. \frac{1}{2} - R^- \right|_{\{\text{GRV LO, } \sin^2 \Theta_W=0.2227\}} = 0.2192(3) \quad (4.7)$$

$$\left. \frac{1}{2} - R^- \right|_{\{\text{GRV NLO, } \sin^2 \Theta_W=0.2227\}} = 0.2192(2) \quad (4.8)$$

$$\left. \frac{1}{2} - R^- \right|_{\{\text{CTEQ NLO, } \sin^2 \Theta_W=0.2227\}} = 0.2196(9) \pm 0.0005(1) . \quad (4.9)$$

The numbers in parentheses are the next digit in the numerical evaluation. For the evaluation of R^- , in addition to the values for $R^{\nu,\bar{\nu}}$ in Table VII one also needs the values for

$$r \equiv \frac{\sigma_{\text{CC}}^{\bar{\nu}}}{\sigma_{\text{CC}}^{\nu}} \quad (4.10)$$

in Table VIII giving

$$R^- = \frac{R^\nu - rR^{\bar{\nu}}}{1 - r} . \quad (4.11)$$

The difference between the numerical values in Eqs. (4.7) and Eqs. (4.8) reflects the impact of a LO or NLO evaluation of the cross sections entering R^- . It is actually beyond the numerical precision of our calculation which is about 10^{-4} . The error quoted with the NLO evaluation using CTEQ6M refers to the master formula (3) in Ref. [34] and has to be understood as explained in detail in this reference. For the observable R^- we find a very robust stability under NLO corrections even under the non-ideal conditions of a non-isoscalar target and in a world of massive charm quarks and a massive target. We also find a similar stability with regards to PDF variations as long as they do not exploit any new physical degree of freedom such as isospin violations or an asymmetry $(s - \bar{s})(x)$ in the strange sea. From theory alone we cannot investigate if the correlations between R^ν and $R^{\bar{\nu}}$ in the analysis [12] are correctly represented by the combined ratio R^- . The values in Eqs. (4.7) - (4.9), nevertheless, support the expectation that the NuTeV anomaly is not a technical NLO effect.

V. SUMMARY

In oscillation searches, neutrino cross sections relate event rates with neutrino fluxes or the absence of events with bounds on oscillation parameters. A recent measurement of the Weinberg angle which deviates from the standard model expectation is based on the observation of neutrino interactions on iron. Contrary to the photon exchange case, the massive boson propagator is non-divergent at vanishing invariant boson mass. Neutrino cross sections are, therefore, dominated by perturbative interactions with quarks and gluons provided the neutrino energy is high enough. The dominance of deep inelastic interactions typically sets in already above a few GeV neutrino energy. Typical Q^2 values are not high

enough, though, to rely on the lowest order parton model picture for anything but a crude estimate. Subleading power suppressed terms and logarithmic corrections are unlikely to be separable in the data and have to be considered on the same footing in theory. In this article we have revisited, summarized and extended the inclusion of perturbative NLO corrections and heavy quark as well as lepton and target mass terms into the twist-2 component of weak structure functions and perturbative neutrino cross sections. Further corrections not considered here are then, by definition, either of NNLO perturbative accuracy or of higher twist. A factor which we have barely discussed here and which does not seem to lend itself to a systematic treatment easily is the impact of our imperfect knowledge of parton distribution functions. Obviously, this is even more true for higher twist parton correlations. This article may be seen as a technical basis and starting point to address some of these points in more detail in the future. We have set up a Monte Carlo integration program for weak structure functions and integrated cross sections and, for now, provided numerical results for two warm-up applications: First, we have investigated the accuracy of target mass corrections in the approximate collinear parton model which we found to be better than 10% for F_2 and better than 20% for F_3 . This result is interesting for computational efficiency and as an expectation for the accuracy of similar approximations to processes where the OPE is not applicable. Second, we have looked into observables that are related to the measurement of the weak mixing angle in neutrino scattering. Though we confirmed the expected stability of the Paschos-Wolfenstein relation, our first results do not allow any final conclusion on the impact of corrective terms to an experimental analysis based on a different cross section model. Future work will be done along this direction which will also take PDF uncertainties into account.

NOTE ADDED ON MOMENT ESTIMATES

After we submitted this article, in addition to Refs. [14, 36] analytic moment estimates of NLO corrections to neutrino cross sections were also presented in Ref. [37]. The authors point out a different sign for the NLO correction to R^ν than we find. Under the same approximations^{***} and conventions^{†††} as used in [37], we reproduce the results in Eqs. (5.14) and (5.15) of that paper. We have then taken the approximate moment approach as a starting point and examined the implications of the different approximations it makes. First, we find that the sign of the NLO correction to R^ν is not flipped by the hadronic energy cut [12] in Eq. (4.3). The hadronic energy cut was not included in [37]. Some of the other approximations made in [37], however, can flip the sign of the correction to R^ν and thus explain the seeming discrepancy between our calculation and that of [37].

^{***}The approximations required for making moment estimates and obtaining energy-independent ratios $R^{\nu,\bar{\nu}}$ are: (i) neglect of evolution, (ii) $M_{Z,W} \rightarrow \infty$ limit of the boson propagator, (iii) neglect of the hadronic energy cut.

^{†††}I.e., to reproduce Ref. [37] we switch to the 4 flavor DIS factorization scheme ($m_c = 0$) adopted there, instead of our canonical 3 flavor $\overline{\text{MS}}$ convention ($m_c \neq 0$).

An approximation that has implications for the sign of the NLO correction to R^ν is the moment approximation itself. The exact μ dependence of the parton distribution functions and coefficient functions is parametrically of order $\alpha_s^2(\overline{Q^2}) \ln(Q^2/\overline{Q^2})$ (for average $Q^2 \equiv \overline{Q^2}$) but its neglect overestimates (underestimates) typical Q values at low x (large x) where structure functions are larger (smaller) for increasing Q . This leads to an overestimate of neutrino cross-sections of about $\sim 10\% - 15\%$ around $E_\nu = 100$ GeV. In addition, for fixed parton distributions (or their second moments), there is a factorization scheme dependence in the NLO correction and a comparison of different conventions is of limited physical significance. Also, the classification of LO and NLO terms is generally not the same for $n_f = 3$ or $n_f = 4$ active parton flavours. We find that both the $Q \simeq \overline{Q}$ approximation and the dependence on the factorization scheme conventions are capable of flipping the sign of the NLO correction to R^ν . More relevant of course than the volatile sign of this correction is the question – posed in [37] and above in Section IV B – of what impact a complete and consistent QCD treatment of neutrino cross sections has on the analysis of the data in Ref. [12]. More detailed numerical results related to NuTeV observables will be presented in a future publication [38].

ACKNOWLEDGMENTS

We thank B. Dobrescu, K. Ellis, K. McFarland, W. Marciano, S. Moch, F. Olness, W.-K. Tung and G. Zeller for discussions and correspondence and G. Zeller also for providing us with tabulated values of the NuTeV neutrino fluxes. S.K. is grateful to RIKEN, Brookhaven National Laboratory and the U.S. Department of Energy (contract No. DE-AC02-98CH10886) for providing the facilities essential for the completion of this work. The work is also supported by the U.S. Department of Energy under Contract No. FG02-91ER40664. M.H.R. thanks the Aspen Center for Physics for its hospitality.

APPENDIX A: GENERAL DIS CROSS SECTIONS

The electroweak weights in Eq. (2.8) for a general $(v_l - a_l)$ leptonic current are given by

$$w_1 = \frac{E_l y [(m_1^2 + 4m_2 m_1 + m_2^2 + 2E_l M x y) a_l^2 + v_l^2 (m_1^2 - 4m_2 m_1 + m_2^2 + 2E_l M x y)]}{4M(E_l^2 - m_1^2)} \quad (\text{A1})$$

$$w_2 = -\frac{[4(y-1)E_l^2 + 2MxyE_l + (m_1 + m_2)^2] a_l^2 + v_l^2 [4(y-1)E_l^2 + 2MxyE_l + (m_1 - m_2)^2]}{8(E_l^2 - m_1^2)} \quad (\text{A2})$$

$$w_3 = -\frac{a_l v_l E_l [-m_1^2 + m_2^2 + 2E_l M x (y-2)] y}{4M(E_l^2 - m_1^2)} \quad (\text{A3})$$

$$w_4 = \frac{a_l^2 [(m_1 - m_2)^2 + 2E_l M x y] (m_1 + m_2)^2 + v_l^2 (m_1 - m_2)^2 [(m_1 + m_2)^2 + 2E_l M x y]}{8M^2(E_l^2 - m_1^2)x} \quad (\text{A4})$$

$$w_5 = -\frac{E_l [(m_1 + m_2)(m_2 + m_1(y-1)) a_l^2 + v_l^2 (m_1 - m_2)(y m_1 - m_1 - m_2)]}{2M(E_l^2 - m_1^2)} \quad (\text{A5})$$

For CC neutrino scattering ($v_l = a_l = 1$, $m_1 = 0$) this reduces to

$$w_1 = \frac{m_2^2 y}{2ME_l} + xy^2 \quad (\text{A6})$$

$$w_2 = 1 - \frac{m_2^2}{4E_l^2} - \left(1 + \frac{Mx}{2E_l}\right) y \quad (\text{A7})$$

$$w_3 = -\frac{m_2^2 y}{4ME_l} + \frac{x}{2}(2-y)y \quad (\text{A8})$$

$$w_4 = \frac{m_2^4}{4E_l^2 M^2 x} + \frac{m_2^2 y}{2ME_l} \quad (\text{A9})$$

$$w_5 = -\frac{m_2^2}{ME_l} \quad (\text{A10})$$

In the above Eqs. (A6)-(A10) one has $m_2 = m_\tau$ for tau neutrinos and for electron or muon neutrinos $m_2 = m_{e,\mu} \simeq 0$. For NC interactions ($m_1 = m_2 = m$) we have

$$w_1 = \frac{E_l y [m^2(3a_l^2 - v_l^2) + E_l M(a_l^2 + v_l^2)xy]}{2(E_l^2 - m^2)M} \quad (\text{A11})$$

$$w_2 = -\frac{E_l v_l^2 [2E_l(y-1) + xyM] + a_l^2 [2m^2 + 2E_l^2(y-1) + E_l Mxy]}{4(E_l^2 - m^2)} \quad (\text{A12})$$

$$w_3 = -\frac{v_l a_l E_l^2 x (y-2)y}{2(E_l^2 - m^2)} \quad (\text{A13})$$

$$w_4 = \frac{a_l^2 E_l m^2 y}{M(E_l^2 - m^2)} \quad (\text{A14})$$

$$w_5 = -\frac{a_l^2 E_l m^2 y}{M(E_l^2 - m^2)} \quad (\text{A15})$$

where $m = 0$ for neutrino neutral current scattering. For charged lepton electromagnetic interactions the w_i in Eqs. (A11)-(A15) with $\{a_l, w_{i>2}\} = 0$, $v_l = 1$ have to be inserted into Eq. (2.10).

TABLES

TABLE I. Coefficients A_j^i in Eq. (3.17).

A_j^i	$i = 1$	$i = 2$	$i = 3$	$i = 4$	$i = 5$
$j = 1$	$\frac{x}{\xi\rho}$	0	0	0	0
$j = 2$	0	$\frac{x^2}{\rho^3\xi^2}$	0	0	0
$j = 3$	0	0	$\frac{x}{\rho^2\xi}$	0	0
$j = 4$	0	$\frac{\mu^2 x^3}{\rho^3}$	0	$\frac{1}{(1+\mu\xi^2)}$	$-\frac{2\mu x^2}{\rho^2}$
$j = 5$	0	$-\frac{\mu x^2}{\rho^3\xi}$	0	0	$\frac{x}{\rho^2\xi}$

TABLE II. Coefficients B_j^i in Eq. (3.17).

B_j^i	$i = 1$	$i = 2$	$i = 3$	$i = 4$	$i = 5$
$j = 1$	0	$\frac{\mu x^2}{\rho^2}$	0	0	0
$j = 2$	0	$\frac{6\mu x^3}{\rho^4}$	0	0	0
$j = 3$	0	0	$\frac{2\mu x^2}{\rho^3}$	0	0
$j = 4$	0	$\frac{-2\mu^2 x^4}{\rho^4}(2 - \mu\xi^2)$	0	0	$\frac{\mu x^2}{\rho^3}$
$j = 5$	0	$\frac{2\mu x^2(1-\mu\xi x)}{\rho^4}$	0	0	$\frac{\mu x^2}{\rho^3}$

TABLE III. Coefficients C_j in Eq. (3.17).

C_1	C_2	C_3	C_4	C_5
$\frac{2\mu^2 x^3}{\rho^3}$	$\frac{12\mu^2 x^4}{\rho^5}$	0	$\frac{2\mu^2 x^3}{\rho^5}(1 - 2\mu x^2)$	$\frac{6\mu^2 x^3}{\rho^5}$

TABLE IV. Coefficients α_j^i in Eq. (3.27).

α_j^i	$i = 1$	$i = 2$	$i = 3$	$i = 4$	$i = 5$
$j = 1$	$\frac{x}{\xi\rho}$	0	0	0	0
$j = 2$	0	$\frac{2x^2}{\lambda\rho^3\xi}$	0	0	0
$j = 3$	0	0	$2\frac{x}{\rho^2\xi}$	0	0
$j = 4$	0	$\frac{2\mu^2\xi^2x^2}{\lambda\rho^2(1+\mu\xi^2)}$	0	$\frac{1}{(1+\mu\xi^2)}$	$-\frac{2\mu x\xi}{\rho(1+\mu\xi^2)}$
$j = 5$	0	$-\frac{2\mu x^2}{\lambda\rho^3}$	0	0	$\frac{x}{\rho^2\xi}$

 TABLE V. Coefficients β_j^i in Eq. (3.27).

β_j^i	$i = 1$	$i = 2$	$i = 3$	$i = 4$	$i = 5$
$j = 1$	0	$\frac{2\mu x^2}{\lambda\rho^2}$	0	0	0
$j = 2$	0	$\frac{12\mu x^3}{\lambda\rho^4}$	0	0	0
$j = 3$	0	0	$\frac{4\mu x^2}{\rho^3}$	0	0
$j = 4$	0	$-\frac{4\mu^2 x^4}{\lambda\rho^4}(2 - \mu\xi^2)$	0	0	$\frac{2\mu x^2}{\rho^3}$
$j = 5$	0	$\frac{4\mu x^2(1-\mu\xi x)}{\lambda\rho^4}$	0	0	$\frac{2\mu x^2}{\rho^3}$

 TABLE VI. Coefficients γ_j in Eq. (3.27).

γ_1	γ_2	γ_3	γ_4	γ_5
$\frac{4\mu^2 x^3}{\lambda\rho^3}$	$\frac{24\mu^2 x^4}{\lambda\rho^5}$	0	$\frac{4\mu^2 x^3}{\lambda\rho^5}(1 - 2\mu x^2)$	$\frac{12\mu^2 x^3}{\lambda\rho^5}$

PDF ($\sin^2 \Theta_W$)	R^ν	$R^{\bar{\nu}}$
GRV NLO (0.2227)	0.3120 (0.3120)	0.3844 (0.3845)
GRV LO (0.2227)	0.3125	0.3860
GRV NLO (0.2277)	0.3088	0.3839
CTEQ6 NLO (0.2227)	0.3105 ± 0.0006	0.3841 ± 0.0038

TABLE VII. The ratios $R^{\nu,\bar{\nu}}$ as defined in Eq. (4.4) evaluated for different parton distributions [33, 34], at leading and higher order and for two values of the Weinberg angle. The error quoted for the CTEQ6 PDF refers to the master formula (3) in [34] and must be understood as explained in detail in this reference. In the first line, the numbers in parentheses refer to a perturbative expansion of the ratios $R^{\nu,\bar{\nu}}$ directly (instead of the ratios of perturbatively expanded cross sections in Eq. (4.4)); i.e. schematically $R^\nu = R_{(0)}^\nu + \alpha_s R_{(1)}^\nu$ inside the parentheses.

PDF	r
GRV NLO	0.3009
GRV LO	0.3014
CTEQ6 NLO	0.2909

TABLE VIII. The ratio r as defined in Eq. (4.10) evaluated for different parton distributions [33, 34], at leading and higher order.

FIGURES

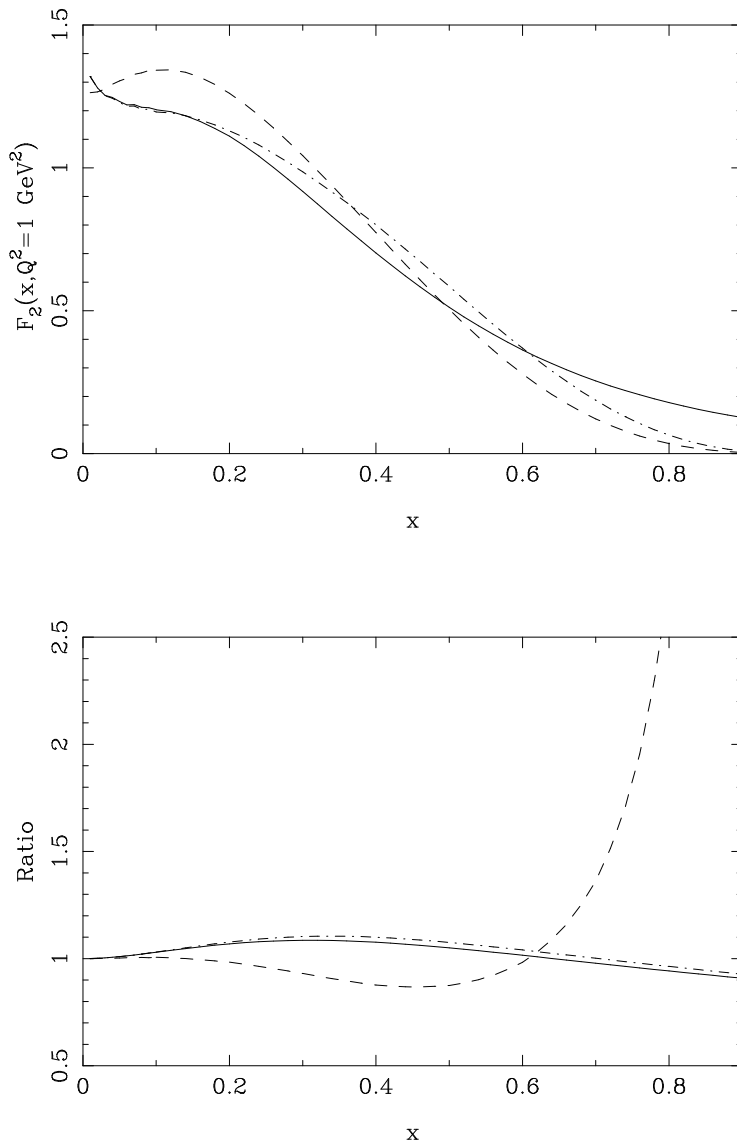


FIG. 1. (a) The charged current neutrino structure function F_2 at $Q^2 = 1 \text{ GeV}^2$ evaluated with NLO ξ -scaling corrections (solid line) and in LO (dashed) and NLO (dot-dashed) under the neglect of target mass corrections. (b) Ratio of the LO ξ -scaling evaluation of F_2 as in (a) with $Q^2 = 1 \text{ GeV}^2$ to the LO evaluation in the collinear approximation is shown by the solid line. The dot-dashed line shows the same ratio at NLO. The dashed line shows the ratio of the NLO target mass corrected F_2 to the NLO F_2 in the $M \rightarrow 0$ limit.

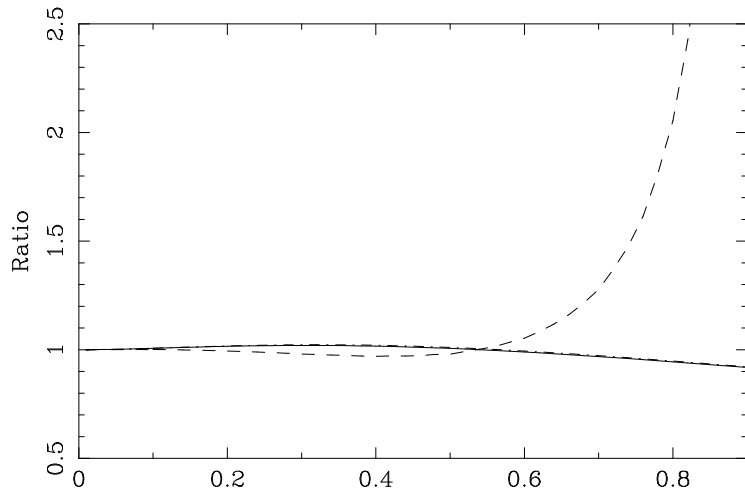
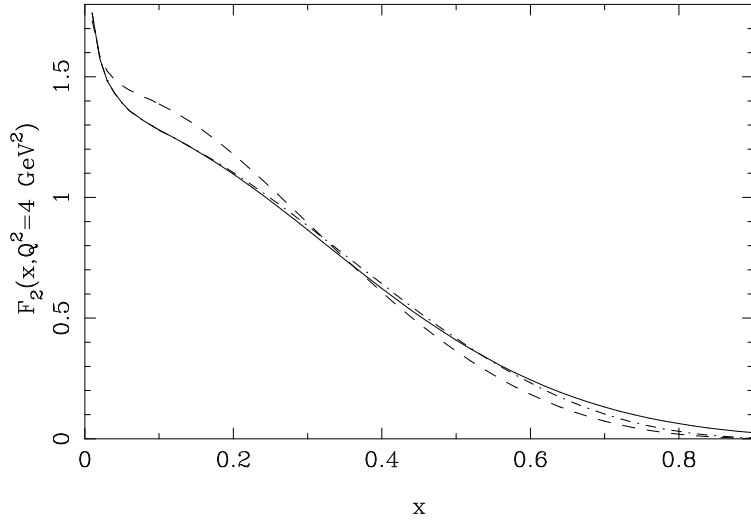


FIG. 2. Same as Fig. 1 for $Q^2 = 4 \text{ GeV}^2$.

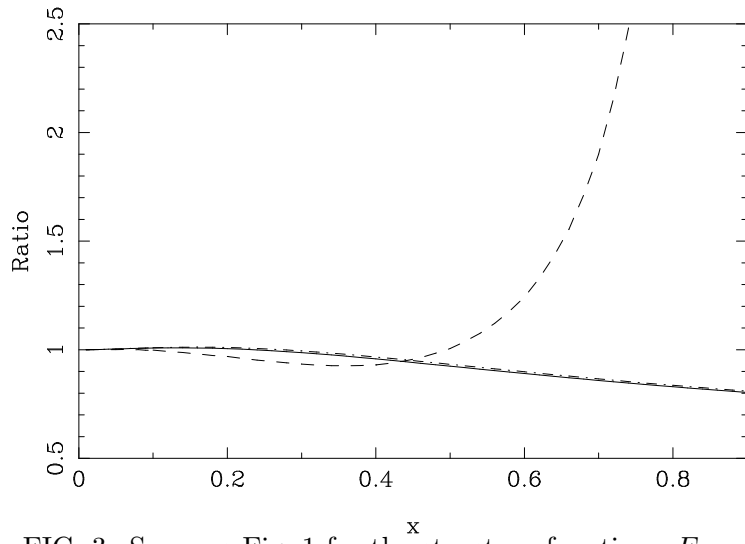
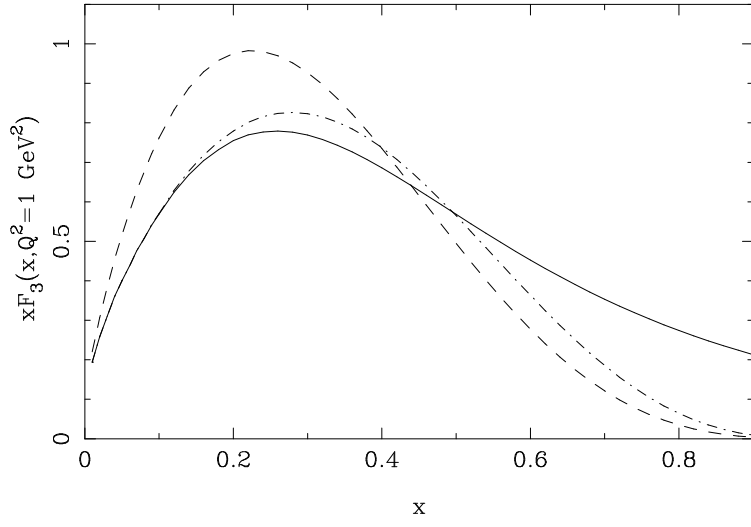


FIG. 3. Same as Fig. 1 for the structure function $x F_3$.

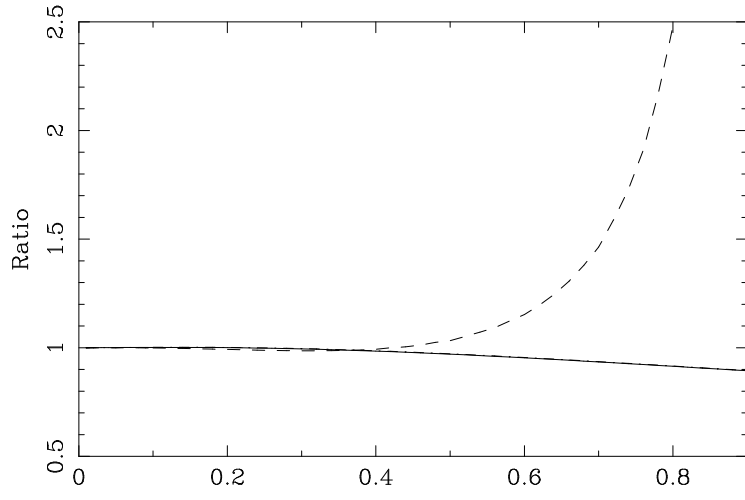
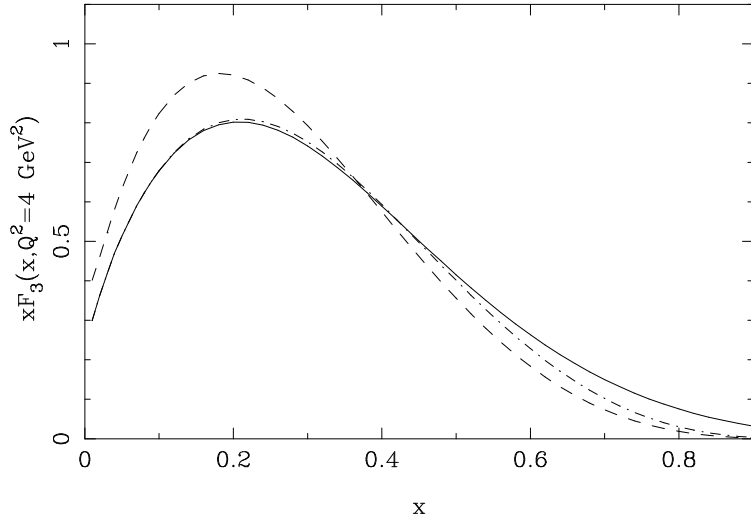


FIG. 4. Same as Fig. 3 for $Q^2 = 4 \text{ GeV}^2$.

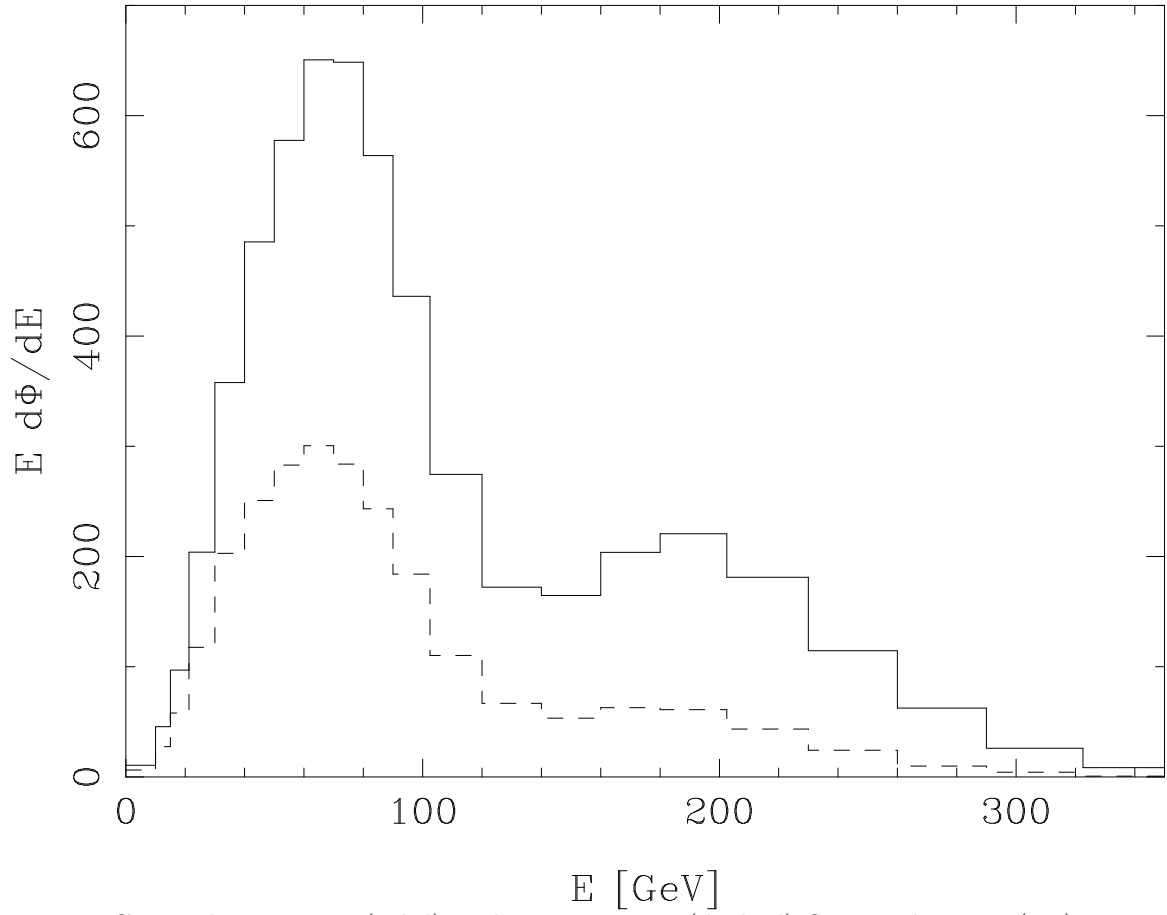


FIG. 5. The neutrino (solid) and anti-neutrino (dashed) flux used in Eq. (4.3).

REFERENCES

- [1] Y. Fukuda *et al.* [Super-Kamiokande Collaboration], Phys. Rev. Lett. **81**, 1562 (1998) [arXiv:hep-ex/9807003].
- [2] Q. R. Ahmad *et al.* [SNO Collaboration], Phys. Rev. Lett. **89**, 011302 (2002) [arXiv:nucl-ex/0204009].
- [3] J. N. Bahcall, M. C. Gonzalez-Garcia and C. Pena-Garay, JHEP **0207**, 054 (2002) [arXiv:hep-ph/0204314].
- [4] M. Maltoni, T. Schwetz, M. A. Tortola and J. W. Valle, Phys. Rev. D **67**, 013011 (2003) [arXiv:hep-ph/0207227].
- [5] See in, for example, J. N. Bahcall, *Neutrino Astrophysics*, Cambridge University Press, 1989.
- [6] A. Rubbia, Nucl. Phys. Proc. Suppl. **91**, 223 (2000) [arXiv:hep-ex/0008071]; F. Arneodo *et al.* [ICARUS and NOE Collaboration], “ICANOE: Imaging and calorimetric neutrino oscillation experiment,” LNGS-P21/99, INFN/AE-99-17, CERN/SPSC 99-25, SPSC/P314; M. Guler *et al.* [OPERA COLLABORATION] CERN/SPSC 2000-028, SPSC/P318, LNGS-P25/2000; F. Terranova [MONOLITH Collaboration], Int. J. Mod. Phys. A **16S1B**, 736 (2001) V. Paolone, Nucl. Phys. Proc. Suppl. **100**, 197 (2001).
- [7] C. H. Llewellyn Smith, Phys. Rept. **3**, 261 (1972).
- [8] P. Lipari, M. Lusignoli and F. Sartogo, Phys. Rev. Lett. **74**, 4384 (1995) [arXiv:hep-ph/9411341].
- [9] E. A. Paschos and J. Y. Yu, Phys. Rev. D **65**, 033002 (2002) [arXiv:hep-ph/0107261].
- [10] H. M. Gallagher and M. C. Goodman, NuMI note NuMI-112 (1995), http://www.hep.anl.gov/ndk/hypertext/numi_notes.html.
- [11] See contributions to *NUINT'02*, Irvine CA (2002); www.ps.usi.edu/~nuint; proceedings to appear in 2003 and contributions to the proceedings of *NUINT'01*, Tsukuba (2001), Nucl. Phys. Proc. Suppl. **112**. These contributions also serve a complete resource of further references.
- [12] NuTeV Collaboration, G.P. Zeller *et al.*, Phys. Rev. Lett. **88**, 091802, 2002.
- [13] D. Abbaneo *et al.*, hep-ex 0112021.
- [14] See e.g.:
S. Davidson, S. Forte, P. Gambino, N. Rius, A. Strumia, JHEP **0202**, 037, 2002.
A full list of references with possible interpretations of Ref. [12] is beyond the scope of the present publication.
- [15] As a point of entry, see e.g.:
A.L. Kataev, *La Thuile 2001, Results and perspectives in particle physics*, 205-221, hep-ph/0107247; J.T. Londergan, A.W. Thomas, hep-ph/0301147; S. Kumano, Phys. Rev. D **66**, 111301 (2002); S. Kovalenko, I. Schmidt, J.-J. Yang, Phys. Lett. B **546**, 68 (2002).
- [16] S. Schäfer, A. Schäfer and M. Stratmann, Phys. Lett. B **514**, 284 (2001).
- [17] H. Georgi and H. D. Politzer, Phys. Rev. D **14**, 1829 (1976).
- [18] R. K. Ellis, W. Furmanski and R. Petronzio, Nucl. Phys. B **212**, 29 (1983).
- [19] A. De Rújula, H. Georgi, and H. D. Politzer, Ann. Phys. **103**, 315 (1977).
- [20] O. Nachtmann, Nucl. Phys. B **63**, 237 (1973).
- [21] M.A.G. Aivazis, F.I. Olness and W.-K. Tung, Phys. Rev. D **50**, 3085 (1994).

- [22] S. Kretzer and M. H. Reno, Phys. Rev. D **66**, 113007 (2002) [arXiv:hep-ph/0208187].
- [23] C. H. Albright and C. Jarlskog, Nucl. Phys. B **84**, 467 (1975).
- [24] K. Wilson, Phys. Rev. **179**, 1499 (1969).
- [25] F.J. Ynduráin, *The Theory of Quark and Gluon Interactions*, Springer Verlag 1983; T. Muta, *Foundations of Quantum Chromodynamics*, World Scientific 1987; M.E. Peskin and D.V. Schroeder, *An Introduction to Quantum Field Theory*, Addison-Wesley 1995.
- [26] S. Wandzura, Nucl. Phys. B **122**, 412 (1977).
- [27] S. Matsuda, T. Uematsu, Nucl. Phys. B **168**, 181 (1980).
- [28] A. Piccione, G. Ridolfi, Nucl. Phys. B **513**, 301 (1998).
- [29] J. Blümlein, A. Tkabladze, Nucl. Phys. B **553**, 427 (1999).
- [30] S. Wandzura and F. Wilczek, Phys. Lett. B **72**, 5 (1977).
- [31] G. Altarelli, R. K. Ellis and G. Martinelli, Nucl. Phys. B **157**, 461 (1979); T. Gottschalk, Phys. Rev. D **23** (1981) 56; W. Furmanski and R. Petronzio, Z. Phys. C **11**, 293 (1982); M. Glück, R.M. Godbole and E. Reya, Z. Phys. C **38** (1988) 441; **39** (1988) 590 (E). M. Glück, S. Kretzer and E. Reya, Phys. Lett. B **380**, 171 (1996); B **405**, 391 (1996) (E).
- [32] M. Luo, J.W. Qiu, G. Sterman, Phys.Rev. D **50**, 1951 (1994).
- [33] M. Glück, E. Reya and A. Vogt, Eur. Phys. J. C **5**, 461 (1998) [arXiv:hep-ph/9806404].
- [34] J. Pumplin, D. R. Stump, J. Huston, H. L. Lai, P. Nadolsky and W. K. Tung, JHEP **0207**, 012 (2002).
- [35] E.A. Paschos and L. Wolfenstein, Phys. Rev. D **7**, 91 (1973).
- [36] K.S. McFarland and S.-O. Moch, hep-ph/0306052.
- [37] B.A. Dobrescu and R.K. Ellis, hep-ph/0310154.
- [38] S. Kretzer and M. H. Reno, in preparation.